The use of equations of state of pure components in pore fluid and fluid inclusion research: Computer program *Pures* (software package *FLUIDS*)

Ronald J. Bakker

Resource Mineralogy, Department of Applied Geosciences and Geophysics, Montanuniversity Leoben, Leoben, Austria

ARTICLE INFO

ABSTRACT

Fluid inclusions and pore fluids seldomly contain pure fluids, i.e. single component, and the properties of these natural fluids must be investigated with complex equations of state for fluid mixtures. However, the properties of nearly-pure fluids can be modelled with equations of state for pure gas components, including an insignificant error. Occasionally, fluid inclusions are observed that can be modelled according to these considerations. The program "*Pures*" has been developed to calculate properties of pure gases: H_2O, CO_2, CH_4, N_2, C_2H_6, O_2, NH_3, CO, H_2, D_2O, Ar, C_3H_8, SO_2, H_2S, and He. These fluid components belong to the most abundant volatile species that are observed in fluid inclusions in quartz and other host minerals in rock. The thermodynamic properties of these fluids are calculated with highly accurate Helmholtz energy functions that cover both the liquid and vapour. Viscosity and surface tension are calculated with additional purely- and semi-empirical equations. Stand-alone applications can be operated in Macintosh-, Windows-, and Linux-based operated computer systems, and contain algorithms that are designed with BASIC language within the XOJO programming environment. A series of twelve self-instructive interfaces (modules) are leading the user through the complex calculation procedures. The modules include the calculation of pressure, temperature, molar volume, isochores, isotherms, fugacity, homogenization conditions, liquid-vapour equilibria, thermodynamic state properties, viscosity, and surface tension. Fluid densities in quartz-confined inclusions can be corrected for temperature- and pressure-dependent volume changes of the host crystal. Fluid modelling in the program "*Pures*" is not restricted to fluid inclusion research, and can also be applied to other research fields that involve a fluid phase. "*Pures*" is included in the software package *FLUIDS*.

1. Introduction

Equations-of-state (EoS) describing the behaviour of fluids according to the parameters temperature, pressure, density and composition are of major importance to the interpretation of fluid properties in inclusions in crystals and pore spaces in rock. Abundant EoS are available and readily used in water management (e.g. Sleep, 1995; Kunst et al., 2002), CO_2 sequestration (e.g. Marini, 2007; Narinesingh and Alexander, 2014), H_2 storage (e.g. Eller et al., 2022), petroleum engineering (e.g. Danish, 1998), sedimentary rock (e.g. Goltapeh et al., 2022), metamorphic and igneous rock (e.g. Liebscher and Heinrich, 2007), and fluid inclusions (e.g. Bakker and Brown, 2003).

The main analytical technique to determine the properties of fluids in inclusions in crystals is microthermometry (e.g. Shepherd et al., 1985): the temperatures of phase changes are directly related to density and compositional properties. Microthermometry includes only the estimation of major components in the fluid phase, such as H_2O, CO_2,

CH_4 and NaCl. The identity of individual gas species is obtained by Raman spectroscopy (e.g. Burke, 2001). Raman spectroscopy also offers the possibility to estimate the density of vapour phases (e.g. Frezzotti et al., 2012; Le et al., 2021 and references therein). However, Bakker (2021) illustrated that this method and resulting equations fail to have sufficient precision and accuracy.

The observations described in the preceding paragraph give abundant data that must be treated with EoS to obtain values of density and composition of the analyzed fluid inclusions (e.g. Bakker, 2009). The large number of available EoS of fluid phases have variable complexity, and have evolved to highly accurate mathematical equations since van der Waals (1873) published his kinematic theory on the behaviour of gas molecules (see also the program "*LonerW*" in Bakker, 2009). The so-called cubic EoS (named after the cubic form of the equation in terms of volume) were classified as "improved" van der Waals type equations (e.g. Redlich and Kwong, 1949; Soave, 1972; Peng and Robinson, 1976; see also Bakker, 2012). A different type of the mathematic formulation

of the behaviour of fluids is the virial EoS, which is based on theory of statistical mechanics, and uses an infinite series of density or the inverse of molar volume, which is usually truncated after the third coefficient. These equations are in general only limited applicable, usually to a limited range of temperatures and pressures. EoS are constantly improved with purely empirical fitting procedures to new experimental data by adding arbitrary and physically meaningless parameters (e.g. Benedict et al., 1940; Lee and Kesler, 1975; Duan et al., 1992a). The main objective of these improvements is to make EoS suitable for both relatively low-density vapour phases, and relatively high-density liquid phases in addition to super-critical fluids. Moreover, the equations must be able to represent both pure fluid phases and fluid mixtures. The latter is being constantly addressed in ongoing research. For example, the highly variable composition of petroleum reservoir fluids needs well-defined mixing rules of fluids, that may vary from nearly pure CH_4 to mixtures of abundant hydrocarbon compounds.

Fluid inclusions contain multiple components such as a variety of gases (e.g. CO_2, CH_4, N_2, H_2), and salts (e.g. NaCl, $CaCl_2$) in addition to the main component H_2O. Apparently, EoS of pure fluids are not of interest to fluid inclusion research. However, the use of highly accurate EoS for pure fluids is twofold: 1. they form the basis for the development for binary, ternary or higher component systems (e.g. Driesner and Heinrich, 2007). 2. they are directly applicable to fluid inclusions that contain nearly pure fluids in separate phases.

A general assumption in the analyses of fluid inclusions is that a gas-bearing vapour bubble in the presence of an aqueous liquid solution is nearly free of salts and water. Consequently, the properties of this vapour bubble are modelled with EoS that describe pure gases, such as CO_2, CH_4, N_2 and H_2, or mixtures of these gases. EoS of pure fluids can be directly applied to monophase gas inclusions, that contain pure CH_4 (e. g. Bakker et al., 2020), pure CO_2 (e.g. Kleinefeld and Bakker, 2002; Frezzotti and Touret, 2014), pure N_2 (e.g. Andersen et al., 1995), and pure H_2 (e.g. Bakker and Elburg, 2006).

The most accurate EoS for pure fluids are defined by Helmholtz energy functions (e.g. Wagner and Pruss, 2002). Density and temperature are the variables within these functions, which can be used to calculate a number of thermodynamic parameters (e.g. pressure, fugacity, enthalpy, entropy, internal energy, Gibbs energy, chemical potentials, heat capacity) according to thermodynamic definitions, fundamental equations, Maxwell relations, and identities (e.g. Prausnitz et al., 1986; Bakker, 2009). The complexity of the mathematical formulations of Helmholtz energy EoS does not allow a simple approach in the calculation procedures, and automated algorithms in newly developed software with user friendly interfaces may greatly facilitate the use of these EoS. Highly accurate unified Helmholtz energy functions for pure fluids are bundled in the present work in the stand-alone program "*Pures*", that is developed for Macintosh, Windows and Linux, using BASIC computer language with the developer software XOJO (XOJO Inc., n.d). The gases involved in this software are listed in Table 1. Some of them were already presented in the original package "*FLUIDS*" (Bakker, 2003) with a simple I/O interface. The selection of gases involves fluid systems that have been observed in fluid inclusions.

2. Method: new program "*Pures*" in the packages "*FLUIDS*"

The program "*Pures*" includes twelve individual windows (modules), that can be used to calculated temperature-pressure-density (*T-p-V*) properties of pure fluids in addition to fugacity, viscosity, surface tension and other thermodynamic state properties. The primary window "*Start*" (Fig. 1) introduces the general fluid model (Helmholtz energy functions) that is used to calculate fluid properties, in addition to a list of 15 pure fluid components (see Table 1) that are included in this software. The second window "*Procedures*" (Fig. 2) is used to select one specific fluid component and one of the nine calculation procedures (modules). These include the calculation of: 1. pressure as a function of temperature and density; 2. molar volume (density) as a function of

Table 1

Fluid components and corresponding references included in the program "*Pures*". The "*Loner*" equivalents illustrate previously published software in Bakker (2003). The max. *Saturation conditions* correspond to the upper temperature and pressure limits of calculation of the saturation curve with the equal-fugacity method (see module "*Bubble-Dew Point*"). The programs "*Loner14*", "*Loner18*", and "*Loner19*" are also available as "*Loner HKG*", "*Loner SpW*", and "*Loner SeW*", respectively, at the website of the Fluid Inclusion Laboratory Leoben (https://fluids.unileoben.ac.at).

component	reference	Loner equivalent Bakker (2003)	max. Saturation conditions	
			T_h (K)	P_h (MPa)
H_2O	Haar et al. (1984) Wagner and Pruss (1993)	Loner14	646.51	21.830
H_2O	Wagner and Pruss (2002) IAPWS R6–95 (International Association for the Properties of Water and Steam, IAPWS R6-95., 2018)		646.49	22.064 (c)
CO_2	Span and Wagner (1996)	Loner18	304.05	7.350
CH_4	Setzmann and Wagner (1991)	Loner19	190.54	4.592 (c)
N_2	Jacobsen et al. (1986)	Loner22	126.16	3.392
N_2	Span et al. (2000)		126.192 (c)	3.395
C_2H_6	Friend et al. (1991)	Loner20	305.32	4.866
C_2H_6	Bücker and Wagner (2006)		305.29	4.861
O_2	Stewart et al. (1991)	Loner35	154.581 (c)	5.043 (c)
NH_3	Haar and Gallagher (1978)	Loner29	404.26	11.148
NH_3	Tillner-Roth and Baehr (1993) Baehr and Tillner-Roth (1995)	Loner36	405.38	11.300
CO	Goodwin (1985)	Loner28	129.15	2.960
CO	Lemmon and Span (2006)		132.35	3.488
D_2O	Hill et al. (1982)		642.82	21.490
D_2O	Herrig et al. (2018)IAPWS R16-17 (2018)		643.64	21.560
H_2 (normal)	Leachman et al. (2009)		32.87	1.245
H_2 (para)	Leachman et al. (2009)		32.67	1.237
H_2 (ortho)	Leachman et al. (2009)		32.93	1.255
C_3H_8	Miyamoto and Watanabe (2000)		369.823 (c)	4.2407
C_3H_8	Lemmon et al. (2009)		369.881 (c)	4.250
SO_2	Lemmon and Span (2006)		429.88	7.863
SO_2	Gao et al. (2016)		429.76	7.771
H_2S	Sakoda and Uematsu (2004)		373.31	8.95
H_2S	Lemmon and Span (2006)		370.34	8.710
Ar	Tegeler et al. (1999)		150.66	4.861
He	Ortiz-Vega (2013)		5.18	0.2248

temperature and pressure; 3. temperature as a function of density and pressure; 4. isochores; 5. isotherms; 6. fugacity; 7. homogenization conditions; 8. liquid-vapour equilibria; and 9. thermodynamic state properties, including internal energy, enthalpy, entropy, Helmholtz energy, Gibbs energy, heat-capacity (C_V and C_P), speed of sound, Joule-Thomson coefficient, and viscosity. The surface tension of pure gasses is also included at saturation conditions in module 7 and 8. Details of the reference and temperature-pressure limits of the selected fluid component are illustrated in the lower right corner of Fig. 2.

The temperature can be defined in °Celsius or Kelvin in each module. A fractional number must be introduced with a decimal point (dot) in each interface, for example, a temperature of 151.4 °C must be defined as "151.4". Molar volume is defined in $cm^3 \cdot mol^{-1}$, and density in $kg \cdot m^{-3}$. The internal energy, enthalpy, Helmholtz energy, and Gibbs energy can be presented in $J \cdot mol^{-1}$ or $kJ \cdot kg^{-1}$, entropy and heat capacities in $J \cdot mol^{-1} \cdot K^{-1}$ or $kJ \cdot kg^{-1} \cdot K^{-1}$. Speed of sound is given in $m \cdot s^{-1}$,
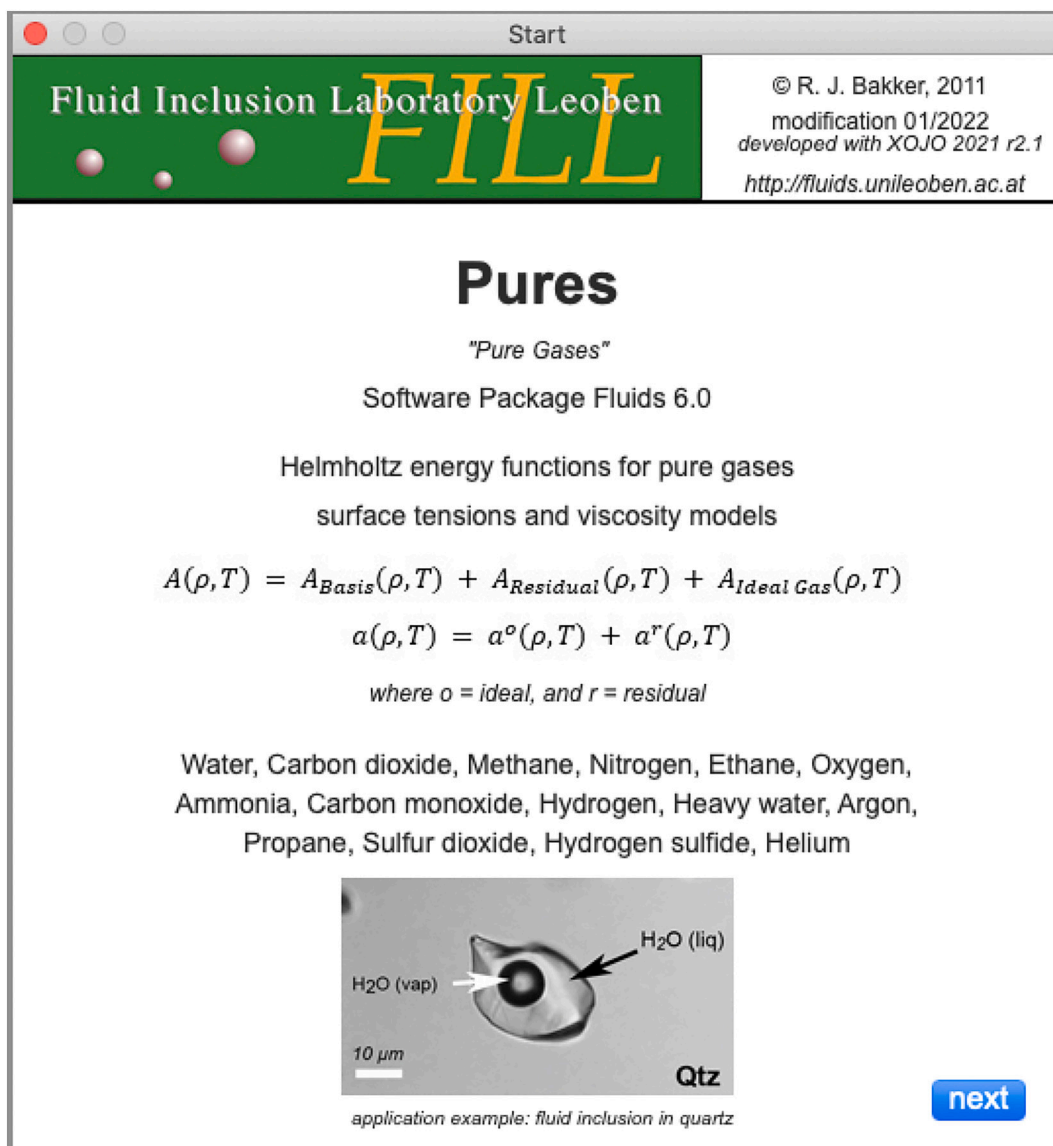
Fig. 1. First window ("*Start*") with which the program "Pures" is opened. This interface is further explained in the text.

Joule-Thomson coefficient in K·MPa^{-1}, viscosity in μPa·s, and surface tension in mN·m^{-1}. Each module contains a "*clear*" button to erase all the introduced and calculated numbers. The number of digits in the fractional part of the calculated properties is not related to the accuracy or precision of that property, but reflects an exact number (floating-point value) calculated in the software development tool of XOJO (https://www.xojo.com).

3. Calculations with pure fluids

3.1. Temperature-pressure-density conditions

Helmholtz energy functions of fluids are defined according to individual components of specific molecular interaction parameters (Eq. 1):

$$a(\varrho, T) = a^o(\varrho, T) + a^r(\varrho, T) \qquad (1)$$

where a is the molar Helmholtz energy (J·mol^{-1}), ϱ is density (kg·m^{-3}), and T is temperature (Kelvin). The superscripts "*o*" and "*r*" reflect the ideal and residual part of the Helmholz energy function, respectively (e. g. Wagner and Pruss, 2002). All the other thermodynamic parameters can be derived from this function by a number of partial derivations

towards volume (or density) and temperature. The Helmholtz energy equation is often defined in a dimensionless form (α) using reduced parameters (Eq. 2):

$$\alpha(\delta, \tau) = \frac{a(\varrho, T)}{RT} \qquad (2)$$

where R is the gas constant (8.314472 J·mol^{-1}·K^{-1}), δ is the reduced density (ϱ/ϱ_C), τ is the invers reduced temperature (T_C/T), the subscript "C" represents the critical point. The symbol ϕ is often used for the dimensionless Helmholtz energy, but is omitted in this study because the same symbol can be used for fugacity coefficients.

The pressure as a function of ϱ and T is related to the Helmholtz energy function according to:

$$p(T, V) = -\left(\frac{\partial A}{\partial V}\right)_{T,n} \qquad (3a)$$

$$p(\varrho, T) = \varrho^2 \left(\frac{\partial A}{\partial \varrho}\right) \qquad (3b)$$

$$p(\delta\tau) = \varrho RT \cdot \left[1 + \delta \left(\frac{\partial \alpha^r}{\partial \delta}\right)_\tau\right] \qquad (3c)$$
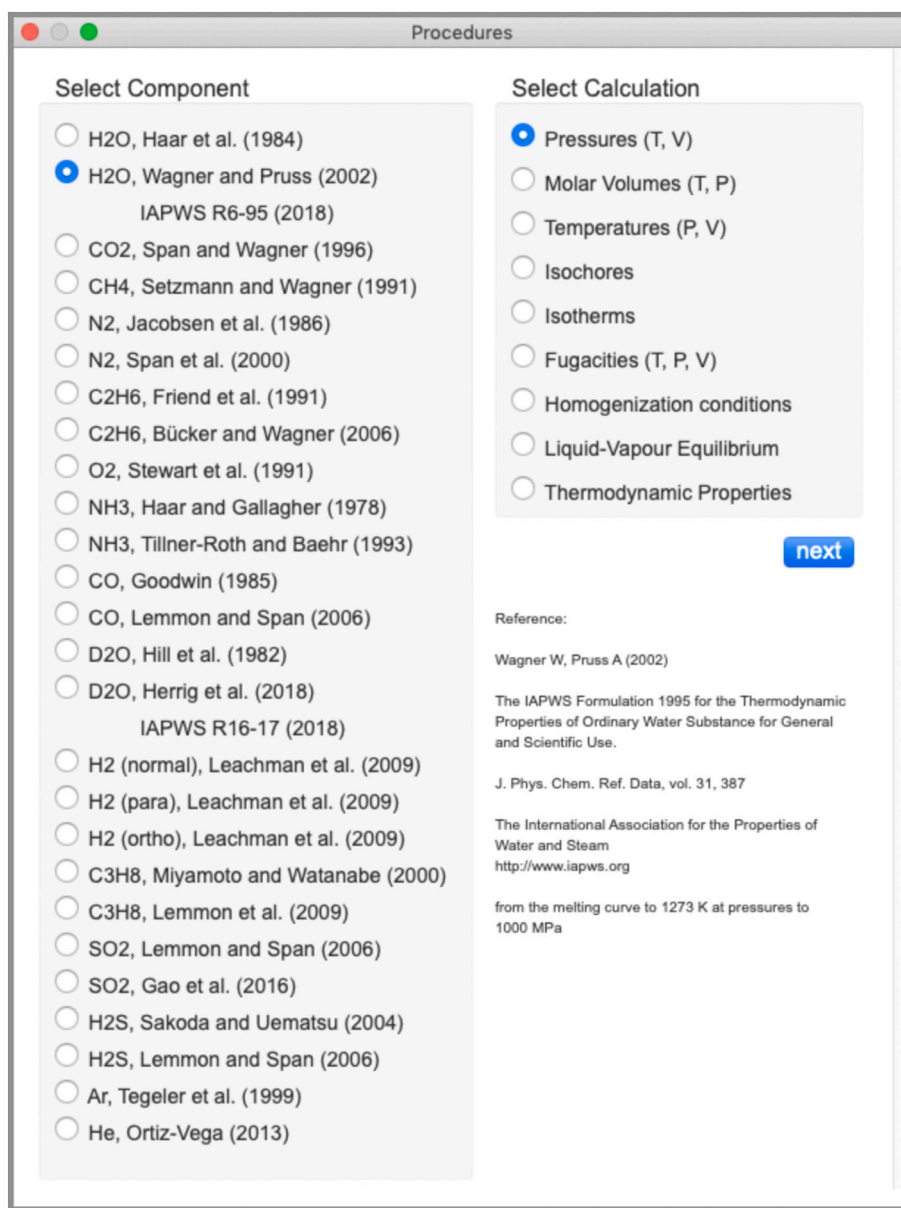
Fig. 2. The second interface "*Procedures*" that is opened with the button"next" in the preceding interface "*Start*". See text for further details.

where p is pressure (MPa), A is the total Helmholtz energy (J), V is the total volume (m^3), n is the amount of substance (mole), and α^r is dimensionless residual Helmholtz energy (c.f. Eq. 1 and 2). Most references of the fluid components listed in Table 1 have used these definitions to calculate the pressure, except for CO (Goodwin, 1985).

Five modules are included in the software "*Pures*" that use Eq. (3) to calculate pressure (module "*Pressure*", Appendix A, Fig. A.1), molar volume and density (module "*Molar Volume*", Appendix A, Fig. A.2), temperature (module "*Temperature*", Appendix A, Fig. A.3), isochores (module "*Isochore*", Appendix A, Fig. A.4) and isotherms (module "*Isotherm*", Appendix A, Fig. A.5).

The calculation of molar volume (module "*Molar Volume*") is relatively more complex than pressure (module "*Pressure*") because of the complexity of the Helmholtz energy function, and the possibility to have multiple solutions at a selected temperature and pressure. The molar volume can only be obtained with a numerical analysis using the definition of pressure (Eq. 3). The analysis is a root-finding method for complex function, such as the Sectant method, Brent-Dekker's method, and Newton-Raphson method (e.g. Press et al., 1997). At a selected

temperature, a first-guess molar volume is used to calculate a pressure, which is compared to the given pressure. The value of molar volume is subsequently adjusted to minimize the difference between the given and calculate pressure. The calculation of temperature (module "*Temperature*") is based on the same principles as used for the calculation of molar volume. A similar root-finding method is used to calculate temperature as a function of molar volume and pressure.

The module "*Isochore*" (Appendix A, Fig. A.4) may calculate isochoric temperature-pressure conditions. The bubble-point curve and dew-point curve represent the lowest temperature and pressure conditions of a specific isochore for a homogeneous fluid (either liquid-like, vapour-like or super-critical), and correspond to homogenization conditions of liquid and vapour phases in fluid inclusions. It should be noted that the bubble-point and dew-point curve coincide at the same temperature-pressure conditions for unary systems, unlike binary systems. The homogenization conditions can be calculated for a selected molar volume. The isochore is defined in a specific temperature interval, of which the lower and upper limit are manually introduced, in addition to a temperature interval. The pressure of the isochore is calculated

within this interval. A useful tool to fluid inclusion research is the possibility to estimate modifications of the fluid density along an isochore according to expansivity and compressibility of the solid container, i.e. natural quartz (Hosieni et al., 1985). Homogenization conditions (temperature and pressure) or a manually defined temperature along the isochore can be selected as reference conditions ("*starting point*" in Appendix A, Fig. A.4), i.e. conditions that correspond to the selected density. The latter automatically calculates the pressure at the "*starting point*". The corrected isochore corresponds to the so-called "*iso-T_h*" curves of fluid inclusions (e.g. Bakker, 2019). The output of this module can be saved in a text file (.txt format) that contains the selected fluid component with corresponding reference and the selected molar volume and density. Two columns, separated with a comma are listing the temperature and corresponding pressure of the selected isochore if a quartz volume correction is ignored, whereas four columns are illustrated for a corrected isochore. These columns include temperature, pressure, modified molar volume of the homogeneous fluid according to quartz expansivity and compressibility, and the phase-state of quartz (either α- or β-quartz).

A curve at constant temperature is defined by a series of molar volumes and corresponding pressures in the module "*Isotherm*" (Appendix A, Fig. A.5). Temperatures that exceed the critical temperature identifies the fluid as a "*supercritical fluid*", otherwise homogenization conditions are calculated for selected temperatures below the critical point and above the triple point (saturation conditions). The result is given in a table and can be exported in a text file (.txt format), similar to the description in the preceding paragraph, but without a correction due to modifications of a quartz host mineral with fluid inclusions.

3.2. Fugacities, homogenization conditions, and liquid-vapour equilibria

The definition of fugacity of pure gases is seldomly presented in the lists of derivatives of Helmholtz energy functions. The fugacity is related to chemical potentials (e.g. Prausnitz et al., 1986; Gottschalk, 2007) which are directly obtained from a partial derivative of the Helmholtz energy (Eq. 4):

$$\mu_i = \left(\frac{\partial A}{\partial n_i}\right)_{T,V,n_j} \tag{4}$$

where μ is the chemical potential of component i (J·mol^{-1}), A is the total Helmholtz energy (J), n is the amount of substance (mole) of component i or j, V is the total volume (m^3). The fugacity coefficient (symbol φ or ϕ) of individual components is defined by Eq. 5:

$$RT\ln(\varphi_i) = \left(\frac{\partial(n_{total} \cdot a^r)}{\partial n_i}\right)_{V,T,n_j} - RT \cdot \ln(Z) + RT \cdot (Z-1) \tag{5}$$

where a^r is the residual molar Helmholtz energy (J·mol^{-1}), Z is compressibility. The subscript "*total*" refers to the total amount of substance. The fugacity coefficient of pure fluids is directly derived from this equation (Eq. 6):

$$\ln(\varphi) = Z - 1 - \ln(Z) + a^r \tag{6}$$

This equation is equivalent to the definition in Eq. (7), without the use of compressibility:

$$\ln(\varphi) = a^r + \left(\frac{\partial a^r}{\partial \delta}\right)_\tau - \ln\left[1 + \left(\frac{\partial a^r}{\partial \delta}\right)_\tau\right] \tag{7}$$

The fugacity of pure fluid components can be calculated at selected temperature-pressure conditions, or at selected temperature-molar volume conditions (Fig. 3). The former calculates numerically a molar volume at the selected *T-p* conditions, whereas the latter calculates analytically a pressure at the selected *T-V* conditions (c.f. modules "*Pressure*" and "*Molar Volume*").

The homogenization conditions of liquid and vapour phases are

Fig. 3. I/O interface of the module "*Fugacity*" with an example of NH$_3$ illustrating the input possibilities to calculate fugacity defined by either temperature-pressure conditions or temperature-molar volume conditions.

analyzed in the module "*Bubble-Dew Point*" (Fig. 4). The calculation procedure can be directly applied to fluid inclusion research, based on observations of the behaviour of fluid inclusions in microthermometric experiments (e.g. Shepherd et al., 1985; Bakker, 2009). The module offers two possibilities to calculate the properties of fluids at saturation conditions: 1. "*simple correlations*", and 2. "*fugacity equality*". *Simple correlations* are polynomial best-fit curves for pressure, density of liquid and vapour at the saturation curve, defined in the individual references (Table 1). Thermodynamically, homogenization is obtained by solving equilibrium equations of a liquid and vapour phase. The two phases are in thermodynamic equilibrium at a constant temperature and pressure when the fugacity of each component is the same in both phases (Eq. 8).

$$f_i^{vap} = f_i^{liq} \tag{8a}$$

$$\varphi_i^{vap} = \varphi_i^{liq} \tag{8b}$$

where f is fugacity (MPa), φ is fugacity coefficient, i is a specific pure gas. The fugacities in both phases are calculated with the same Helm-

Fig. 4. I/O Interface of the module "*Bubble-Dew Point*" with an example of CO illustrating the input possibilities to calculate the saturation curve (bubble- and dew-point) defined by either equal-fugacity calculations according to Prausnitz et al. (1980) or simple correlation (best-fit polynomials).

holtz energy function. The algorithm of this software is designed to filter irrelevant intersection possibilities. The range of homogenization conditions (*T, p*) in a unary (single-component) system is equal for liquid-rich and vapour-rich inclusions, due to coinciding dew-point curve and bubble-point curve. The bubble-point curve corresponds to homogenization in the liquid phase upon heating the inclusion (LV → L), whereas the dew-point curve corresponds to homogenization in the vapour phase (LV → V). The "*mode*" of homogenization (Fig. 4) illustrates the phase that "disappears" (or dissolves) and is used to obtain the correct solution. The module offers the possibility to select either a temperature or a pressure at homogenization conditions. Subsequently, a homogenization pressure or temperature are calculated, respectively. The "*fugacity equality*" method cannot be applied close to the critical point, due to the inaccuracy of Helmholtz energy functions at these temperatures and due to mathematical difficulties to solve the equations. The limits of these calculation procedures are given in Table 1 for

each gas component. For example, the Lemmon and Span (2006) equation of CO cannot be applied in the range 132.35 to 132.80 K (i.e. critical temperature) to calculate saturation properties where it fails to describe accurately both liquid and vapour phases. Similarly, the Haar et al. (1984) equation for H_2O can only be applied up to 646.51 K (373.36 °C), which is 0.62° below the critical temperature. Levelt-Sengers et al. (1983) provides an equation of state that can be applied to this region, between 643 and 695 K (program "*Loner LKBS*", freeware downloadable at https://fluids.unileoben.ac.at or https://rohmin.unileoben.ac.at/downloads). The range of calculation possibilities at the saturation curve is slightly reduced by these restrictions, which is illustrated in the "*explanation*" button (Fig. 4). An additional feature in this module is the surface tension along the saturation curve, which is calculated with relatively simple purely empirical best-fit equations (Mulero et al., 2012).

The module "*Liquid-Vapour Equilibrium*" performs similar calculation

procedures as in the module "*Bubble-Dew Point*". This module calculates the properties of coexisting liquid and vapour phases below homogenization conditions at the saturation curve (Fig. 5). First, a bulk molar volume (or density) is defined, corresponding to the properties of a homogeneous fluid phase above homogenization conditions. This molar volume corresponds to a specific homogenization temperature that is automatically calculated in the module. Then, a temperature below the homogenization conditions has to be selected, at which the properties of the coexisting phases are calculated, including the surface tension. The volume fractions of each phase are calculated assuming that the inclusions are true isochoric systems.

3.3. Thermodynamic properties

The internal energy, enthalpy, entropy, Helmholtz energy, Gibbs energy, heat capacity at constant volume (C_V), heat capacity at constant pressure (C_P), speed of sound, Joule-Thomson coefficient, and viscosity of pure gases are calculated in the module "*Thermodynamic Properties*" (Fig. 6). Most properties are derived from Helmholtz energy functions, that are illustrated with the "*thermodynamic definitions*" button. More detailed definitions of the relationship between thermodynamic state properties can be examined in e.g. Prausnitz et al. (1986), Gottschalk (2007), or Thorade and Saadat (2013). *V*iscosity is calculated with a variety of semi-empirical models (Table 2), which can be summarized in three types (Eq. 9), in addition to purely empirical formulations (e.g. Giri et al., 2012).

$$\eta(T, V) = \eta_0(T) + \eta_1(T, V) + \eta_2(T, V) \tag{9a}$$

$$\overline{\eta}(T, V) = \overline{\eta_0}(T_r) \times \overline{\eta_1}(T_r, V_r) \times \overline{\eta_2}(T_r, V_r) \tag{9b}$$

$$\eta(T, P) = \eta_0(T) + \eta_1(T, P) \tag{9c}$$

where η_0 in Eq. (9a) and (9b) is the viscosity in the zero-density limit, i.e. dilute gas (Eq. 10), which is defined by particle kinematics according to the Chapman-Enskog theory (e.g. Assael et al., 2014). The subscript "r" and the macron refer to reduced values of temperature, volume, and viscosity. η_1 and η_2 are the residual viscosity and critical contribution, respectively.

$$\eta_0(T) = \frac{5}{16} \cdot \frac{\sqrt{\pi \cdot u \cdot M_r \cdot k_B \cdot T}}{\pi \cdot \sigma^2 \cdot \Omega} \tag{10}$$

Fig. 5. I/O interface of the module "*Liquid-Vapour Equilibrium*" with an example of D$_2$O illustrating the input possibilities to calculate liquid-vapour phase equilibrium at the saturation curve defined by either equal-fugacity calculations according to Prausnitz et al. (1980) or simple correlation (best-fit polynomials).

Fig. 6. I/O interface of the module "*Thermodynamic Properties*" with an example of Ar illustrating the input possibilities to calculate thermodynamic state properties (internal energy, enthalpy, entropy, Helmholtz energy, Gibbs energy, heat capacity, speed of sound, Joule-Thomson coefficient, and viscosity) defined by either temperature-pressure conditions or temperature-molar volume conditions.

Table 2
Fluid components and corresponding references of viscosity models included in the program "*Pures*".

component	reference
H_2O	Haar et al. (1984)
	Quiñones-Cisneros and Deiters (2006)
	Huber et al. (2009)
CO_2	Fenghour et al. (1998)
	Quiñones-Cisneros and Deiters (2006)
CH_4	Friend et al. (1989)
	Quiñones-Cisneros and Deiters (2006)
N_2	Najafi et al. (2000)
	Lemmon and Jacobsen (2004)
C_2H_6	Friend et al. (1991)
	Quiñones-Cisneros and Deiters (2006)
O_2	Najafi et al. (2000)
	Lemmon and Jacobsen (2004)
NH_3	Fenghour et al. (1995)
CO	Najafi et al. (2000)
D_2O	Matsunaga and Nagashima (1983)
	Assael et al. (2021)
H_2 (normal)	Muzny et al. (2013)
C_3H_8	Vogel et al. (1998)Quiñones-Cisneros and Deiters (2006)
H_2S	Schmidt et al. (2008)
	Giri et al. (2012)
Ar	Younglove and Hanley (1986)
	Lemmon and Jacobsen (2004)
He	Arp et al., 1998Najafi et al. (2000)

where u is the unified atomic mass unit (kg), M_r is the molar mass (kg·mol^{-1}), k_B is the Boltzmann constant ($1.380658 \cdot 10^{-23}$ m^2·kg·s^{-2}·K^{-1}), σ is a Lennard-Jones size parameter (m), and Ω is the collision integral. Fenghour et al. (1995), Vogel et al. (1998), and Muzny et al. (2013) defined the constant fraction in front of the square root in Eq. (10) at 4/16. Eq. (9b) is used only for H_2O and D_2O, and Eq. (9c) is defined by the friction theory (e.g. Quiñones-Cisneros and Deiters, 2006). η_0 is a purely empirical equation in Eq. (9b) and (9c). The residual contributions (η_1) are also purely empirical equations, that highly depend on the originally determined η_0. The residual part in Eq. (9c) is defined by the repulsive and attractive pressure term of an EoS. Near the critical point, the viscosity of some components is characterized with an extra term (η_2). The calculated viscosities according to the references in Table 2 may slightly differ from reported values due to inconsistencies in *p-T-V* values. Each viscosity model is designed with knowledge of the density or pressure at a selected temperature, which is defined by a specific EoS that may differ from the selected EoS in this program.

Similar to the module "*Fugacity*", temperature-pressure conditions or temperature-molar volume (density) conditions can be selected (Fig. 6). The former calculates numerically a molar volume at the selected *T-p* conditions. The latter provides directly the parameters that are required to perform the calculations that are used to estimate the pressure and all other thermodynamic state properties with an analytical procedure. The reference state of the thermodynamic properties can be selected according to the definition of the original publications (e.g. ideal gas properties at the triple point), or at 25 °C and 0.1 MPa according to the

standard state values reported in Robie et al. (1979). The latter allows the calculation of energy changes with a common reference state, that is generally applied to heterogeneous reactions with minerals that involve volatile components.

4. Comparable software

Calculation of properties of pure gases have been made accessible in a number of software packages, both online and stand-alone programs. The "NIST Chemistry Webbook" (https://webbook.nist.gov), is a website that allows online calculations of properties of pure fluid components, similar to the calculation procedures in the present work, but without the applications to fluid inclusion research. The NIST Chemistry Webbook is restricted to calculate isotherms, isochores, isobars, and saturation properties, along which the thermodynamic parameters are calculated. The website "The Engineering ToolBox" (https://www.engineeringtoolbox.com) provides only limited possibilities to calculate the properties of pure fluid components in an "online calculator". This website fails to supply the references of the original publications.

Several stand-alone programs (freeware) are provided by Bakker (2003) and Bakker and Brown (2003) and can be downloaded from the website of the Fluid Inclusion Laboratory Leoben (n.d.) (https://fluids.unileoben.ac.at) or the website of Resource Mineralogy of the Montanuniversity Leoben (n.d.) (https://rohmin.unileoben.ac.at/downloads). This software is the precursor of the present study, and was designed with a less flexible I/O interface. The improvements of the present study are the incorporation of more and up-to-data EoS of pure fluids, replacement of a number of single stand-alone programs with one program that includes all the pure gas components, and the use of a user-friendly I/O interface designed with XOJO Inc. (n.d.) (https://www.xojo.com).

A number of commercial software packages are available that may calculate the properties of pure fluid components and fluid mixtures with highly accurate Helmholtz energy functions, such as "*GERG-2008*" and "*FluidCal*", both are available at the website of Wagner at the Ruhr University Bochum (n.d.) https://www.thermo.ruhr-uni-bochum.de/thermo/forschung/wagner_software.html.en. The EoS that are used in "*GERG-2008*" are described in Kunz and Wagner (2012). NIST Chemistry Webbook, n.d provides the software package REFPROP, n.d(https://www.nist.gov/srd/refprop; Lemmon et al., 2018), that includes a large number of fluid components . These commercial packages include the same EoS (Helmholtz energy functions) as those included in the present program "*Pures*". None of these packages include specific calculation procedures for fluid inclusion research. These packages were mainly designed for various Windows operating systems, whereas the present stand-alone software "*Pures*" is designed for a wider variety of operating systems (Windows, MacOs and Linux). The module "*Thermodynamic Properties*" (Fig. 6) in "*Pures*" may replace part of those commercial software packages and the NIST chemistry Webbook.

5. Case studies

5.1. p-T-V-x properties of H_2O-CH_4-rich fluid inclusions

EoS for pure H_2O and pure CH_4 can be used to estimate the bulk fluid properties of H_2O-CH_4-rich fluid inclusions. This can be illustrated with a hypothetical fluid inclusion that contains 60 vol% aqueous solution (nearly pure H_2O), and 40 vol% CH_4-rich vapour bubble at room temperatures. This vapour phase can be treated as a pure CH_4 phase due to the low solubility of H_2O. At low temperatures, the CH_4-rich phase unmix in a CH_4-rich vapour and liquid phase. The partial homogenization of these CH_4-rich phases occurs at −90 °C in the absence of a clathrate (metastable). At this temperature a CH_4 vapour bubble homogenize in a CH_4 liquid phase. First, the EoS of pure CH_4 (Setzmann and Wagner, 1991) is used to calculate the density of the CH_4 phase at partial homogenization conditions: 261.67 kg·m^{-3} or 61.31 cm^3·mol^{-1}

(using module "*Bubble-Dew Point*", Fig. 4). Second, the pressure inside the fluid inclusion at room temperature is calculated according to the isochore of pure CH_4: 43.2 MPa (using module "*Pressure*", Appendix A, Fig. A.1). The aqueous phase wetting the walls of the inclusions is assumed to act as a rigid and inert container of the CH_4 vapour phase. The aqueous solution can be treated as an approximately pure phase (H_2O) due to the low solubility of CH_4. At room temperatures, the density of the H_2O-rich phase can be calculated according to the EoS of pure H_2O (Wagner and Pruss, 2002): 1017.1 kg·m^{-3} or 17.71 cm^3·mol^{-1} (using module "*Molar Volume*", Appendix A, Fig. A.2). Finally, the bulk properties of this fluid inclusion are calculated with volumetric fractions of the individual phases: x(H_2O) = 0.8485 and V_m = 24.75 cm^3·mol^{-1}.

The software "*BULK*" in the package *FLUIDS* (Bakker, 2003; Bakker and Brown, 2003) is also able to do similar calculations, but also includes the mutual solubility of H_2O and CH_4 in both liquid and vapour phases at room temperatures. The properties of the aqueous phase at room temperature are calculated with an EoS for H_2O-CH_4 mixtures (e.g. Duan et al., 1992b), and Henry constants of gas solubility (e.g. Rettich et al., 1981). Subsequently, the bulk properties of the selected example illustrated in the preceding paragraph are calculated at x(H_2O) = 0.835, and a bulk density of 715.56 kg·m^3 (24.722 cm^3·mol^{-1}), which is an insignificant difference from the result calculated without mutual solubilities. It should be noted that both types of analysis include the use of volume fractions of individual phases, and that total homogenization temperatures (i.e. solvus conditions) do not play a role in the calculation of bulk properties, because solvi are not well-defined by EoS for fluid mixtures.

The presence of salt is mainly affecting properties of the aqueous phase. Gas components are "salted-out" and the remaining aqueous phase can be described in a binary H_2O-salt system, whereas the vapour phase can be treated as a pure gas phase.

5.2. p-T-V-x properties of H_2O-CO_2-rich fluid inclusions

A common observation in many fluid inclusion studies is the presence of two fluid phases, i.e. an aqueous liquid phase and a vapour bubble. A hypothetical fluid inclusion (H_2O-CO_2-rich) is used to illustrate a calculation example of bulk fluid properties and isochores using EoS of pure fluids. Microthermometry of the hypothetical inclusion reveals only the final dissolution of ice at −2.0 °C, and eutectic temperatures are not detectable. A clathrate phase is not observed at lower temperatures. The presence of CO_2 in the vapour bubble cannot be verified due to the absence of phase separation at lower temperatures. However, the relatively large vapour bubble (50 vol%) reveals a very weak Raman signal of CO_2. An attemp to analyse total homogenization results in decrepitation.

The software "*BULK*" does not provide a direct solution for this hypothetical inclusion, because the density of the CO_2-rich phase cannot be determined. The Raman spectroscopic analyses may provide a rough value on the density by measuring the wavenumber distance between the two major Raman bands of CO_2 (Fermi doublet), but this method includes a large uncertainty (Bakker, 2021) which largely exceeds uncertainties in volume fraction estimations (Bakker and Diamond, 2006). Another approach to calculate the bulk properties of this inclusion is offered by the software "*CURVES*" in the computer package *CLATHRATES* (Bakker, 1997). Although a clathrate phase was not observed, the quadruple point 1 (Q_1) where a clathrate, CO_2-rich vapour, aqueous liquid, and ice coexist defines the upper pressure limit (about 1 MPa) of ice dissolution conditions in this inclusion (see also Diamond, 2003). The ice melting conditions in the absence of a clathrate (stable) can only occur in the temperature range between the triple point of pure H_2O (0.0 °C) and the Q_1 point (−1.5 °C). The presence of salt in the aqueous solution depresses both temperatures in similar magnitudes. Consequently, a measured dissolution temperature of ice at −2.0 °C may correspond to a salinity range of 0.9 mass% (Q_1) to 3.4 mass% NaCl. The maximum density of the CO_2 vapour phase is calculated at 21 kg·m^3,

corresponding to 2152 cm^3·mol^{-1} (at Q_1). The bulk composition of this fluid inclusion is calculated with volume fractions to a maximum x(CO$_2$) = 0.013, and x(H$_2$O) = 0.984 at Q_1 conditions. The bulk molar volume of this inclusion is 36.52 cm^3·mol^{-1}.

The results can be used to construct an isochore in a temperature-pressure diagram. The nearly pure H$_2$O composition of this inclusion may justify the use of an EoS for pure water (e.g. Wagner and Pruss, 2002) to construct this isochore (using module "*Isochore*", Appendix A, Fig. A.4). At 600 °C, this isochore reaches 143 MPa. The software offers the possibility to correct for the expansivity and compressibility of quartz (i.e. the host mineral of this fluid inclusion), which result in a corrected pressure of 138.6 MPa at 600 °C. These values can be compared to calculations with EoS for ternary H$_2$O-CO$_2$-NaCl fluid mixtures that may represent the actual properties of this inclusion. The uncorrected isochore reaches 131.7 MPa with the Bowers and Helgeson equation, see software "*LonerB*" (Bakker, 2012), and 145.8 MPa with the Duan equation, see software "*LonerAP*" (Bakker, 2023). The difference in pressure is insignificant compared to the uncertainties that can be included in these calculations.

6. Concluding remarks

The use of EoS of pure fluids in fluid inclusion research and pore fluid studies usually implies a simplification of natural fluid properties. The lack of accurate EoS for binary, termary, and more complex fluid mixtures occasionally permits the use of EoS of pure fluids, assuming ideal behaviour of solutions. The magnitude of the error introduced by this simplification can only be estimated by comparison to experimental data of fluid mixtures. Fluid mixtures that contain more than 97 mol% of a specific gas component can be treated as single component pure fluids, that results in only insignificant deviations of fluid properties in most geological environments.

The package "*FLUIDS*" offers abundant possibilities to calculate bulk fluid properties of fluid inclusions, i.e. the sum of all phase within an isolated space in a crystal (Bakker, 2003). The new program "*Pures*" within this package performs calculations only with pure fluid components, and is the successor of part of the original group of "*Loner*" programs (Table 1). The programs can be downloaded from the websites of the Fluid Inclusion Laboratory Leoben (https://fluids.unileoben.ac.at) or the website of Resource Mineralogy of the Montanuniversity Leoben (https://rohmin.unileoben.ac.at/downloads).

Declaration of Competing Interest

The authors declare that they have no known competing financial interests or personal relationships that could have appeared to influence the work reported in this paper.

Data availability

No data was used for the research described in the article.

Appendix A. Supplementary data

Supplementary data to this article can be found online at https://doi.org/10.1016/j.chemgeo.2023.121751.

References

Andersen, T., Burke, E.A.J., Neumann, E.-R., 1995. Nitrogen-rich fluid in the upper mantle: fluid inclusions in spinel dunite from Lanzarote, Canary Islands. Contrib. Mineral. Petrol. 120, 20–28.

Arp, V.D., McCarty, R.D., Friend, D.G., 1998. Thermophysical Properties of Helium-4 from 0.8 to 1500 K with Pressures to 2000 MPa. NIST Technical Note 1334, p. 145.

Assael, M.J., Goodwin, A.R.H., Vesovic, V., Wakeman, W.A., 2014. Advances in Transport Properties of Fluids, Experimental Thermodynamics Volume IX. Royal Society of Chemistry, Cambridge.

Assael, M.J., Monogenidou, S.A., Huber, M.L., Perkins, R.A., Sengers, J.V., 2021. New international formulation for the viscosity of heavy water. J. Phys. Chem. Ref. Data 50, 033102. https://doi.org/10.1063/5.0048711.

Baehr, H.D., Tillner-Roth, R., 1995. Thermodynamic Properties of Environmentally Acceptable Refrigerants. Springer Verlag, Berlin.

Bakker, R.J., 1997. Clathrates: Computer programs to calculate fluid inclusion V-X properties using clathrate melting temperatures. Comput. Geosci. 23, 1–18.

Bakker, R.J., 2003. Package FLUIDS 1. Computer programs for analysis of fluid inclusion data and for modelling bulk fluid properties. Chem. Geol. 194, 3–23.

Bakker, R.J., 2009. Package FLUIDS. Part 3. Correlations between equations of state, thermodynamics and fluid inclusions. Geofluids 9, 63–74.

Bakker, R.J., 2012. Thermodynamic properties and applications of modified van-der-Waals equations of state. In: Morales-Rodriguez, R. (Ed.), Thermodynamics, Fundamentals and its Application in Science, Chapter 7. InTech, Croatia, pp. 163–190.

Bakker, R.J., 2019. Package Fluids. Part 5: the NaCl-H$_2$O system in fluid inclusion research and applications of the software AqSo_NaCl (Bakker, 2018). Chem. Geol. 525, 400–413.

Bakker, R.J., 2021. The perfection of Raman spectroscopic gas densimeters. J. Raman Spectrosc. https://doi.org/10.1002/jrs.6245.

Bakker, R.J., 2023. New developments of the software package FLUIDS: The programs *PURE* and *LonerAP*. In: Caracciolo, A. (Ed.), ECROFI XXVII, Program and Abstract Book, Reykjavik, p. 15.

Bakker, R.J., Brown, P.E., 2003. Computer modelling in fluid inclusion research. In: Samson, I., Anderson, A., Marshall, D. (Eds.), Fluid Inclusions, Analysis and Interpretation, Mineralogical Association of Canada, Short Course, vol. 32, pp. 175–212.

Bakker, R.J., Diamond, L.W., 2006. Estimation of volume fractions of liquid and vapor phases in fluid inclusions, and definition of inclusion shapes. Am. Mineral. 91, 635–657.

Bakker, R.J., Elburg, M.A., 2006. A magmatic-hydrothermal transition in Arkaroola (northern Flinders Ranges, South Australia): from diopside-titanite pegmatites to hematite-quartz growth. Contrib. Mineral. Petrol. 152, 541–569.

Bakker, R.J., Pushkarev, E., Biryuzova, A.P., 2020. High temperature reduced granulite-facies nature of garnetites in the Khabarny Mafic-Ultramafic Massif, Southern Urals: evidence from fluid and mineral analyses. J. Petrol. 1-25 https://doi.org/10.1093/petrology/egaa066.

Benedict, M., Webb, G.B., Rubin, L.C., 1940. An empirical equation for thermodynamic properties of light hydrocarbons and their mixtures I. methane, ethane, propane and n-butane. J. Chem. Phys. 8, 334–345.

Bücker, D., Wagner, W., 2006. A reference equation of state for the thermodynamic properties of ethane for temperatures from the meting line to 675 K and pressures up to 900 MPa. J. Phys. Chem. Ref. Data 35, 205–266.

Burke, E.A.J., 2001. Raman microspectrometry of fluid inclusions. Lithos 55, 139–158.

Danish, A., 1998. PVT and Phase Behaviour of Petroleum Reservoir Fluids. Elsevier, Amsterdam.

Diamond, L.W., 2003. Introduction to gas-bearing, aqueous fluid inclusions. In: Samson, I., Anderson, A., Marshall, D. (Eds.), Fluid Inclusions, Analysis and Interpretation, Mineralogical Association of Canada, Short Course, vol. 32, pp. 101–158.

Driesner, T., Heinrich, C.A., 2007. The system H$_2$O-NaCl. Part I: correlation formulae for phase relations in the temperature-pressure-composition space frpm 0 to 1000 °C, 0 to 5000 bar, and 0 to 1 x_{NaCl}. Geochim. Cosmochim. Acta 71, 4880–4901.

Duan, Z., Møller, N., Weare, J.H., 1992a. An equation of state for the CH$_4$-CO$_2$-H$_2$O system: I. Pure systems from 0 to 1000°C and 0 to 8000 bar. Geochim. Cosmochim. Acta 56, 2605–2617.

Duan, Z., Møller, N., Weare, J.H., 1992b. An equation of state for the CH$_4$-CO$_2$-H$_2$O system: II. Mixtures from 50 to 1000°C and 0 to 1000 bar. Geochim. Cosmochim. Acta 56, 2619–2631.

Eller, J., Sauerborn, T., Becker, B., Buntic, I., Gross, J., Helmig, R., 2022. Modeling subsurface hydrogen storage with transport properties from entropy scaliing using the PC-SAFT equation of state. Water Resour. Res. 58. https://doi.org/10.1029/2021WR030885.

Engineering ToolBox: Resources, Tools and Basic Information for Engineering and Design of Technical Applications. n.d. https://www.engineeringtoolbox.com (accessed 1 August 2023).

Fenghour, A., Wakeham, W.A., Vesovic, V., Watson, J.T.R., Millat, J., Vogel, E., 1995. The viscosity of ammonia. J. Phys. Chem. Ref. Data 24, 1649–1667.

Fenghour, A., Wakeham, W.A., Vesovic, V., 1998. The viscosity of carbon dioxide. J. Phys. Chem. Ref. Data 27, 31–44.

Fluid Inclusion Laboratory Leoben. n.d. https://fluids.unileoben.ac.at (accessed 1 August 2023).

Frezzotti, M.-L., Touret, J.L.R., 2014. CO$_2$, carbonate-rich melts, and brines in the mantle. Geosci. Front. 5, 697–710.

Frezzotti, M.-L., Tecce, F., Casagli, A., 2012. Raman spectroscopy for fluid inclusion analysis. J. Geochem. Explor. 112, 1–20.

Friend, D.G., Ely, J.F., Ingham, H., 1989. Thermophysical properties of methane. J. Phys. Chem. Ref. Data 18, 583–638.
Friend, D.G., Ingham, H., Ely, J.F., 1991. Thermodynamic properties of Ethane. J. Phys. Chem. Ref. Data 20, 275–347.
Gao, K., Wu, J., Zhang, P., Lemmon, E.W., 2016. A Helmholtz energy equation of state for sulfur dioxide. J. Chem. Eng. Data 61, 2859–2872.
Giri, B.R., Marriott, R.A., Blais, P., Wu, Y., 2012. H$_2$S viscosities and densities at high-temperatures and pressures. In: Carroll, J.J., Zhu, W. (Eds.), Sour Gas and Related Technologies. Scrivener Publishing LLC, pp. 37–48.
Goltapeh, S.A., Min, R., Aagaard, P., Hellevang, H., 2022. Extension of SAFT equation of state for fluids confined in nano-pores of sedimentary rocks using molecular dynamic simulation. J. Mol. Liq. 348 https://doi.org/10.1016/j.molliq.2021.118045.
Goodwin, R.D., 1985. Carbon monoxide thermophysical properties from 68 to 1000 K at pressure to 100 MPa. J. Phys. Chem. Ref. Data 14, 849–932.
Gottschalk, M., 2007. Equations of state for complex fluids. In: Liebscher, A., Heinrich, C. A. (Eds.), Fluid-fluid interactions. Reviews in Mineralogy and Geochemistry, vol. 65. Mineralogical Society of America and Geochemical Society, pp. 49–97.
Haar, L., Gallagher, J.S., 1978. Thermodynamic properties of ammonia. J. Phys. Chem. Ref. Data 7, 635–792.
Haar, L., Gallagher, J.S., Kell, G.S., 1984. NBS/NRC Steam Tables. Hemisphere Publishing Corporation, Washington, New York, London.
Herrig, S., Thol, M., Harvey, A.H., Lemmon, E.W., 2018. A Reference Equation of State for Heavy Water. J. Phys. Chem. Ref. Data 47, 043102. https://doi.org/10.1063/1.5053993.
Hill, P.G., MacMillan, R.D.C., Lee, V., 1982. A fundamental equation of state for heavy water. J. Phys. Chem. Ref. Data 11, 1–14.
Hosieni, K.R., Howald, R.A., Scanlon, M.W., 1985. Thermodynamics of the lambda transition and the equation of state of quartz. Am. Mineral. 70, 782–793.
Huber, M.L., Perkins, R.A., Laesecke, A., Friend, D.G., Sengers, J.V., Assael, M.J., Metaxa, I.N., Vogel, E., Mares, R., Miyagawa, K., 2009. New international formulation for the viscosity of H$_2$O. J. Phys. Chem. Ref. Data 38, 101–125.
International Association for the Properties of Water and Steam, IAPWS R6-95., 2018. Revised Release on the IAPWS Formulation 1995 for the Thermodynamic Properties of Ordinary Water Substance for General and Scientific Use (2018).
International Association for the Properties of Water and Steam, IAPWS R16-17, 2018. Revised Release on the IAPWS Formulation 2017 for the Thermodynamic Properties of Heavy Water (2018).
Jacobsen, R.T., Stewart, R.B., Jahangiri, M., 1986. Thermodynamic properties of nitrogen from the freezing line to 2000 K at pressures to 1000 MPa. J. Phys. Chem. Ref. Data 15, 735–909.
Kleinefeld, B., Bakker, R.J., 2002. Fluid inclusions as microchemical systems: evidence and modelling of fluid–host interactions in plagioclase. J. Metamorph. Geol. 20, 845–858.
Kunst, S., Kruse, T., Burmester, A., 2002. Sustainable Water and Soil Management. Springer, Berlin.
Kunz, O., Wagner, W., 2012. The GERG-2008 wide-range equation of state for natural gases and other mixtures: an expansion of GERG-2004. J. Chem. Eng. Data 57, 3082–3091.
Le, V.-H., Caumon, M.-C., Tarantola, A., 2021. FRAnCIs calculation program with universal Raman calibration data for the determination of PVX properties of CO$_2$-CH$_4$-N$_2$ and CH$_4$-H$_2$O-NaCl systems and their uncertainties. Comput. Geosci. 156 https://doi.org/10.1016/j.cageo.2021.104896.
Leachman, J.W., Jacobsen, R.T., Penoncello, S.G., Lemmon, E.W., 2009. Fundamental equations of state for parahydrogen, normal hydrogen, and orthohydrogen. J. Phys. Chem. Ref. Data 38, 721–747.
Lee, B.I., Kesler, M.G., 1975. A generalized thermodynamic correlation based on three-parameter corresponding states. AICHE J. 21, 510–527.
Lemmon, E.W., Jacobsen, R.T., 2004. Viscosity and thermal conductivity equations for nitrogen, oxygen, argon, and air. Int. J. Thermophys. 25, 21–69.
Lemmon, E.W., Span, R., 2006. Short fundamental equations of state for 20 industrial fluids. J. Chem. Eng. Data 51, 785–850.
Lemmon, E.W., McLinden, M.O., Wagner, W., 2009. Thermodynamic properties of propane. III. A reference equation of state for temperatures from the melting line to 650 K and pressures up to 1000 MPa. J. Chem. Eng. Data 54, 3141–3180.
Lemmon, E.W., Bell, I.H., Huber, M.L., McLinden, M.O., 2018. NIST Standard Reference Database 23: Reference Fluid Thermodynamic and Transport Properties-REFPROP, Version 10.0. National Institute of Standards and Technology, Standard Reference Data Program, Gaithersburg. https://doi.org/10.18434/T4/1502528.
Levelt-Sengers, J.M.H., Kamgar-Parsi, R., Balfour, F.W., Sengers, J.V., 1983. Thermodynamic properties of steam in the critical region. J. Phys. Chem. Ref. Data 12, 1–28.
Liebscher, A., Heinrich, C.A., 2007. Fluid-fluid interactions. In: Reviews in Mineralogy and Geochemistry, vo., 65. Mineralogical Society of America, Geochemical Society.
Marini, L., 2007. Geological sequestration of carbon dioxide, thermodynamics, kinetics, and reaction path modeling. In: Developments in Geochemistry 11. Elsevier, Amsterdam.
Matsunaga, N., Nagashima, A., 1983. Transport properties of liquid and gaseous D$_2$O over a wide range of temperature and pressure. J. Phys. Chem. Ref. Data 12, 933–966.
Miyamoto, H., Watanabe, K., 2000. A thermodynamic property model for fluid phase propane. Int. J. Thermophys. 21, 1045–1072.
Mulero, A., Cachadina, I., Para, M.I., 2012. Recommended correlations for the surface tensions of common fluids. J. Phys. Chem. Ref. Data 41, 043105. https://doi.org/10.1063/1.4768782.

Muzny, C.D., Huber, M.L., Kazakov, A.F., 2013. Correlation for the viscosity of normal hydrogen obtained from symbolic regression. J. Chem. Eng. Data 58, 969–979.
Najafi, B., Ghayeb, Y., Parsafar, G.A., 2000. New correlation functions for viscosity calculation of gases over wide temperature and pressure ranges. Int. J. Thermophys. 21, 1011–1031.
Narinesingh, J., Alexander, D., 2014. CO$_2$ enhanced gas recovery and geological sequestration in condensate reservoir: a simulation study of the effects of injection pressure on condensate recovery from reservoir and CO$_2$ storage efficiency. Energy Procedia 63, 3107–3115.
NIST Chemistry Webbook, SRD 69. n.d. https://webbook.nist.gov (accessed 1 August 2023).
Ortiz-Vega, D.O., 2013. A New Wide Range Equation of State for Helium-4 (Ph.D. Dissertation). A&M University, Texas, USA.
Peng, D.Y., Robinson, D.B., 1976. A new two-constant equation of State. Ind. Eng. Chem. Fundam. 15, 59–64. https://doi.org/10.1021/i160057a011.
Prausnitz, J.M., Anderson, T.F., Grens, E.A., Eckert, C.A., Hsieh, R., O'Connell, J.P., 1980. Computer Calculations for the Multicomponent Vapor-Liquid and Liquid-Liquid Equilibria. Prentice-Hall, Englewood Cliffs, New Jersey.
Prausnitz, J.M., Lichtenthaler, R.N., Gomes de Azevedo, E., 1986. Molecular Thermodynamics of Fluid-Phase Equilibria, 2nd edn. Prentice-Hall Inc., Englewood Cliffs, NJ.
Press, W.H., Teukolsky, S.A., Vetterling, W.T., Flannery, B.P., 1997. Numerical Recipes in C, the Art of Scientific Computing. Cambridge University Press, Cambridge.
Quiñones-Cisneros, S.E., Deiters, U.K., 2006. Generalization of the Friction Theory for viscosity modelling. J. Phys. Chem. B 110, 12820–12834.
Redlich, O.R., Kwong, J.N.S., 1949. On the thermodynamics of solutions, V: an equation of state, fugacities of gaseous solutions. Chem. Rev. 44, 233–244.
REFPROP. NIST Reference Fluid Thermodynamic and Transport Properties Database, Version 10. https://www.nist.gov/srd/refprop (accessed 1 August 2023).
Resource Mineralogy of the Montanuniversity Leoben. n.d. https://rohmin.unileoben.ac.at/downloads. (accessed 1 August 2023).
Rettich, T.R., Handa, Y.P., Battino, R., Wilhelm, E., 1981. Solubility of gases in liquids. 13. High-precision of Henry's constants for methane and ethane on liquid water at 275 to 328 K. J. Phys. Chem. 85, 3230–3237.
Robie, R.A., Hemingway, B.S., Fisher, J.R., 1979. Thermodynamic Properties of Minerals and Related Substances at 298.15 K and 1 Bar (10^5 Pascals) pressure and at higher Temperatures. USGS Bull. 1452 second edition, Washington.
Ruhr University Bochum. n.d. https://www.thermo.ruhr-uni-bochum.de/thermo/forschung/wagner_software.html.en.
Sakoda, N., Uematsu, M., 2004. A thermodynamic property model for the fluid phase hydrogen sulfide. Int. J. Thermophys. 25, 709–737.
Schmidt, K.A.G., Carroll, J.J., Quiñones-Cisneros, S.E., Kvamme, B., 2008. Hydrogen sulphide viscosity modelling. Energy Fuel 22, 3424–3434.
Setzmann, U., Wagner, W., 1991. A new equation of state and tables of thermodynamic properties for methane covering the range from the melting line to 625 K at pressures up to 1000 MPa. J. Phys. Chem. Ref. Data 20, 1061–1155.
Shepherd, T.J., Rankin, A.H., Alderton, D.H.M., 1985. A Practical Guide to Fluid Inclusion Studies. Blackie, Glasgow.
Sleep, B.E., 1995. A method of characteristic model fro equation of state compositional simulation of organic compounds in groundwater. J. Contam. Hydrol. 17, 189–212.
Soave, G., 1972. Equilibrium constants from a modified Redlich-Kwong equation of state. Chem. Eng. Sci. 27, 1197–1203. https://doi.org/10.1016/0009-2509(72)80096-4.
Span, R., Wagner, W., 1996. A new equation of state for carbon dioxide covering the fluid region from the triple-point temperature to 1100 K at pressures up to 800 MPa. J. Phys. Chem. Ref. Data 25, 1509–1596.
Span, R., Lemmon, E.W., Jacobsen, R.T., Wagner, W., Yokozeki, A., 2000. A reference equation of state for the thermodynamic properties of nitrogen for temperatures from 63.151 to 1000 K and pressures to 2200 MPa. J. Phys. Chem. Ref. Data 29, 1364–1433.
Stewart, R.B., Jacobsen, R.T., Wagner, W., 1991. Thermodynamic properties of oxygen from the tripe point to 300 K with pressures to 80 MPa. J. Phys. Chem. Ref. Data 20, 917–1021.
Tegeler, Ch., Span, R., Wagner, W., 1999. A new equation of state for Argon covering the fluid Region for temperatures from the melting line to 700 K at pressures up to 1000 MPa. J. Phys. Chem. Ref. Data 28, 779–850.
Thorade, M., Saadat, A., 2013. Partial derivatives of thermodynamic state properties for dynamic simulation. Environ. Earth Sci. 70, 3497–3503.
Tillner-Roth, R., Baehr, H.D., 1993. Eine neue fundamentalgleichung für Ammoniak. DKV-Tagungsbericht 20, 167–181.
Vogel, E., Küchenmeister, C., Bich, E., 1998. Reference correlation of the viscosity of propane. J. Phys. Chem. Ref. Data 27, 947–970.
Waals van der, J.D., 1873. De continuïteit van den gas- en vloeistoftoestand (Ph. D. dissertation). University Leiden.
Wagner, W., Pruss, A., 1993. International equations for the saturation properties of ordinary water substances. Revised according to the international temperature scale of 1990. Addend. J. Chem. Phys. Ref. Data 16, 783–787.
Wagner, W., Pruss, A., 2002. The IAPWS formulation 1995 for the thermodynamic properties of ordinary water substance for general and scientific use. J. Phys. Chem. Ref. Data 31, 387–535.
XOJO. n.d. https://www.xojo.com (accessed 1 August 2023).
Younglove, B.A., Hanley, H.J.M., 1986. The viscosity and thermal conductivity coefficients of gaseous and liquid argon. J. Phys. Chem. Ref. Data 15, 1323–1337.